Digital Simulation Model for Brine Coning
in Unconfined Anisotropic Aquifers

S. P. Rajagopalan and U. V. Jose

Centre for Water Resources Development and Management,
Calicut 673 571 Kerala, India

A digital simulation model has been presented for locating the steady state stable brine cone position beneath partially penetrating wells tapping from the fresh water zone overlying a saline zone in an unconfined anisotropic aquifer. A graphical procedure developed by Morris Muskat has been converted into a numerical one and is used to successively approximate the brine cone position. The truncation in the fresh water zone both due to the brine cone and the depression in the water table are taken care of by repeated adjustment of the hydraulic conductances of the affected branches in the numerical model of the aquifer. An iterative version of the alternating direction implicit method has been used to solve the flow equations repeatedly till successively modified fresh water flow zones converge within a specified tolerance level. The results from the simulation model for a range of expected field conditions of aquifer, well and fluid density contrast have been presented in the form of graphs making use of appropriate non-dimensional parameters. These results can find applications in designing wells so that the discharge from those wells are limited to levels below which fresh water alone is drawn without any contamination by the underlying salt water.

Introduction

Unconfined aquifers in which fresh water floats over saline water is encountered in many places. The fresh water in such places can be tapped by wells partially penetrating the fresh water zone. This induces an upward coning of the salt water – fresh water interface which in turn may lead to the contamination of the pumped

water if the apex of the cone reaches the bottom of the well. This problem is referred to as brine coning.

The first reported solution to a problem similar to the one under consideration is by Muskat (1937, 1949), who gave a graphical procedure for determining the position of the steady state stable interface position for water coning beneath an oil well. Benett, Mundorff and Amjad Hussain (1968) have reported an electric analog model solution coupled with Muskat's graphical procedure for locating the steady state stable brine cone position. The electric analog model used in their study was equipped with a system of switches by which the lower boundary of the network which simulates the aquifer could be adjusted to take care of the truncation of the fresh water zone by the brine cone. Thus it was possible to successively approximate the lower boundary position of the fresh water zone. In using analytic expressions Muskat however found it necessary to assume that the fresh water head distribution as given by the analytic expressions which he used was unaffected by the coning. Other reported work on the brine coning problem are those by Bear and Dagan (1968), Schmorak and Mercado (1969) and Kemblowski (1985).

There is however considerable scope for additional work. For instance, Muskat's graphical procedure can itself be converted into a numerical one, and solved more elegantly with the aid of a digital computer. The advantages so gained would be also substantially preserved if a computer aided digital model is used for solving the flow equations. These are achieved in the study reported in this paper. The reduction in the fresh water zone due to depression in the free surface was not considered in the electric analog model solution. This has also been incorporated in this study. The digital model is also more flexible to take care of heterogeneous aquifer systems especially those in which a low permeability clay layer occurs between the screen bottom and the brine interface.

Mathematical Model

Assumptions

Some of the significant assumptions which have been made while formulating the mathematical model are presented below:

a) The unconfined aquifer is homogeneous and exhibits simple two-dimensional anisotropy with the principal axes of anisotropy coinciding with the r and z axes of the cylindrical co-ordinate system.

b) The well which is co-axial with the z axis is of finite diameter and partially penetrates the fresh water zone. The storage volume within the well is however negligible and is ignored. The well is pumped at a constant discharge.

c) The steady state flow is achieved when the well discharge Q is sustained by a recharge I which is distributed uniformly over the aquifer upto the radius of

44

influences r_e. Hence we have the relation $Q = \pi r_e^2 I$. In this problem the water is removed from storage at water table depths has been approximated to represent the recharge I. Thus the recharge I is not from any external source and we are only considering vertical component of flow. The reduction in the fresh water zone because of water removal from the water table depths can be taken care of by successive modifications of the free surface elevations. This has been achieved in the digital model described later.

d) The flow entering the well from the aquifer is uniform over the screened segment of the well and there is no head loss as flow passes through the well screen. The digital simulation model described later can however take care of the well losses by artifically assigning a relatively less permeability to the aquifer segment close to the well screen.

e) The salt water is static and groundwater flow which is confined within the fresh water zone obeys Darcy's law and exhibits radial symmetry above the well axis.

f) The fresh water-salt water interface is horizontal over the area of influence of the well prior to pumping. Also, the fresh water heads are the same throughout the aquifer prior to pumping.

g) In brine coning problems, there will be in actual practice a mixing zone between the fresh and salt water and the well may be threatened by this mixing zone long before salt water enters the well. Such mixing can be promoted by pumping and is mainly due to dispersion. This aspect has been however ignored in the present study and a sharp interface between fresh and salt water has been assumed.

Equations of Flow

The aquifer, well and flow conditions can be represented in the two dimensional $r - z$ plane as shown in Fig. 1. Based on assumptions a) and e) listed above, the differential equation governing the flow in the fresh water zone can be derived as (Neuman 1974)

$$P_r \left(\frac{\partial^2 h}{\partial r^2} + \frac{1}{r} \frac{\partial h}{\partial r} \right) + P_z \frac{\partial^2 h}{\partial z^2} \equiv 0 \tag{1}$$

The boundary conditions may be stated as follows

i) along the free surface (based on assumption c) listed above)

$$P_r \frac{\partial H}{\partial r} \frac{\partial h}{\partial r} - P_z \frac{\partial h}{\partial z} + \frac{\sim Q}{\pi r_e^2} \equiv 0 \tag{2}$$

ii) along the well screen face (based on assumption d) listed above)

$$\frac{\partial h}{\partial r} = \frac{Q}{2 \pi r_w P_r (z_t - z_b)} \qquad \text{over} \quad z_b \leq z \leq z_t \tag{3a}$$

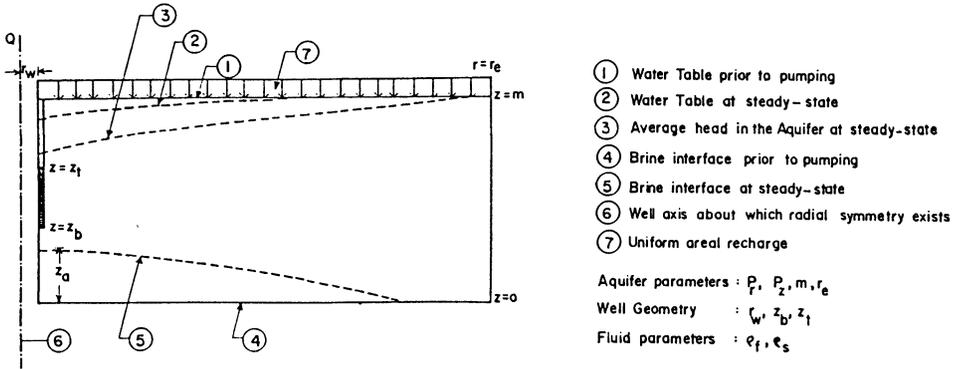$$= 0 \qquad \text{over} \quad 0 \leq z < z_b \; ; \text{ and} \quad z_t < z \leq m \tag{3b}$$

45

Fig. 1. Definition sketch of aquifer, well and flow conditions.

iii) along $r = r_e$ over all z

$$\frac{\partial h}{\partial r} \equiv 0 \qquad\qquad (4)$$

iv) along the brine cone whose position is actually to be determined

$$\frac{\partial h}{\partial n} = 0 \qquad\qquad (5)$$

Notation

List of symbols used

H	– Head at water table during steady state	L
I	– Uniformly distributed recharge	LT^{-1}
P_r	– Permeability of the aquifer in the radial direction	LT^{-1}
P_z	– Permeability of the aquifer in the vertical direction	LT^{-1}
Q	– Constant well discharge	$L^3 T^{-1}$
h	– Hydraulic head in the aquifer at steady state. It is a function of r and z	L
h_o	– Head in the aquifer at steady state at the point $z = m$ and $r = r_e$	L
h_w	– Average head in the well screen segment at steady state	L
h'	– Fresh water head on the brine interface at the radius of influence of the well	L
m	– Initial thickness of the freshwater zone	L
n	– Coordinate normal to brine interface	L
r	– Radial coordinate	L
r_e	– Radius of influence of well	L
r_w	– Radius of well	L
z	– Vertical coordinate	L
z_a	– Elevation of apex of brine cone	L
z_b	– Elevation of bottom of well screen	L
z_t	– Elevation of top of well screen	L
ϱ_f	– Density of fresh water	$M L^{-3}$
ϱ_s	– Density of salt water	$M L^{-3}$
$\triangle\varrho$	– Density difference $(\varrho_s - \varrho_f)$	$M L^{-3}$

46

Density Interface Relationship

Along the brine cone in addition to Eq. (5), the following density interface relationship as given by Hubbert (1940) is also to be satisfied

$$h \equiv h' - \frac{\Delta\rho}{\rho_f} z \tag{6}$$

Dimensionless Form

The elevation z and radial coordinate r at any point may be non-dimensionalised as z/h_o and r/r_e respectively. The hydraulic head h at any point may be non-dimensionalised as $(h-h_w)/(h_o-h_u)$. A dimensionless parameter hereafter referred to as "Flow net constant" can be defined as equal to $(P_r/P_z)(h_o/r_e)^2$. The well geometry can be defined by three dimensionless parameters r_w/r_e, z_t/h_o and z_b/h_o. It can then be easily shown that the model results of fresh water heads and elevations of stable brine cone in dimensionless form would apply equally well to any situation as long as the flow net constant and the dimensionless parameters of the well geometry are identical. If the above condition is satisfied it can be also easily shown that for given values of h_o-h_w, the model results would apply equally well to any situation as long as two dimensionless parameters defined by $Q/(h_oP_r(h_o-h_w))$ and $(\Delta\rho/\rho_i)(h_o/(h_o-h_w))$ are also identical. The dimensionless parameter $Q/(h_oP_r(h_o-h_w))$ will hereafter be referred to as dimensionless specific capacity term and is of interest to the extent that it permits the calculation of well discharge associated with a given brine coning situation. The other dimensionless term $(\Delta\rho/\rho_f)(h_o/h_o-h_w))$ is in fact the slope of Eq. (6) expressed in dimensionless form. Since this equation will be referred to again in the section on numerical scheme of Muskat's graphical procedure, the dimensionless form of Eq. (6) alone is given below

$$\frac{h - h_w}{h_0 - h_w} \equiv \frac{h' - h_w}{h_0 - h_w} - \frac{\Delta\rho}{\rho_f} \frac{h_0}{(h_0 - h_w)} \frac{z}{h_0} \tag{7}$$

Digital Simulation Model

The digital simulation model which has been developed in this study to seek a solution of the mathematical model is an integration of the following three components:

i) Several trials of numerical solution of the flow equations for successively modified fresh water zone.

ii) A numerical scheme of Muskat's graphical procedure to successively modify the lower boundary of the fresh water zone.

iii) A numerical scheme to take care of the truncation in the fresh water zone due to successive modifications of the lower boundary and due to the depression in the free surface.

These three components are described briefly here.

Numerical Solution of the Flow Equations

The aquifer is discretised in the numerical model as a system of co-axial cylindrical shells. This discretised system can be represented as a two-dimensional finite difference grid with nodes along columns occurring at equally spaced intervals $\triangle z$. These columns are placed at radii being a constant multiple α of the preceeding ones. Each branch in the grid represents an aquifer segment. The hydraulic conductance of an aquifer segment in a given direction can be defined as equal to the product of the permeability in that direction, and area of cross section to flow divided by the length of flow. Each branch in the grid can be assigned its hydraulic conductance value based on the above definition. A relationship of the form $a = \log_e r$ can be substituted and Eq. (1) can be rewritten as

$$\frac{P_r}{r^2} \frac{\partial^2 h}{\partial a^2} + P_z \frac{\partial^2 h}{\partial z^2} = 0 \qquad (8)$$

The finite difference approximation of Eq. (8) can then be directly written in terms of the hydraulic conductance assigned to the branches in the finite difference grid. The vertical recharge as discussed earlier is simulated at the nodes in the top most row with the flow rate at each node being proportional to area to vertical flow represented by that node, and the summation of all such flow rates being equal to the well discharge. The discharge from the well is simulated at those nodes in the inner most column which represents the well screen with the discharge rate at each of those nodes being proportional to the screen segment represented by those nodes.

The implicit finite difference equations at all the nodes give rise to a system of simultaneous equations which can be solved using the alternating direction implicit (ADI) method. The computing algorithm is a modification of the iterative version reported by Prickett and Lonnquist (1971) for the case of unsteady state flow in the cartesian co-ordinate system. Such modifications required for the steady state flow in the radial co-ordinate system have been reported by Lakshminarayana and Rajagopalan (1977).

Numerical Scheme for Muskat's Graphical Procedure

Let the dimensionless heads at all the nodes in the grid as obtained from the solution of the flow equation be designated as $H_{i,j}$. A set of co-ordinates comprising of values of $H_{1,j}$ at nodes along the inner most column of the grid beneath the well screen and the corresponding dimensionless elevations z_j/h_o can be then obtained. Let there be NBW such co-ordinates.

In Muskat's graphical procedure a curve has to be first fitted passing through the NBW set of co-ordinates. The general shape of the curve will be as shown in Fig. 2. Then the slope of the line as shown in Fig. 2, which is tangential to the fitted curve
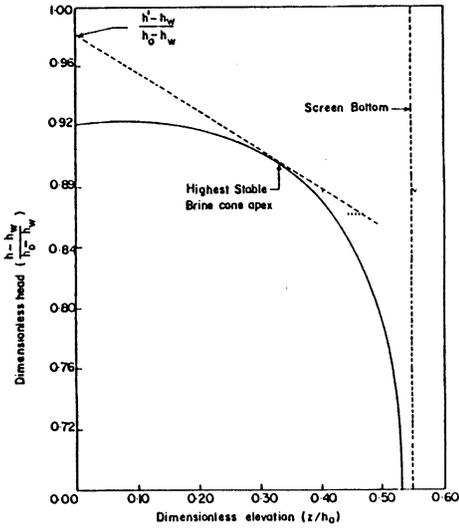
Fig. 2. Illustration of Muskat's Graphical Procedure.

Table 1 – Sample calculation for fitting the curve in Muskat's Graphical Procedure.

Results Apply for: $(P_r/P_z)\,(h_o/r_e)^2 = 0.12$; $r_e/r_w = 2{,}896$; $z_b/h_o = 0.35$; $z_t/h_o = 0.95$
Number of co-ordinates available for fitting the curve, NBW $= 4$

j	Ordinates from the solution of Flow Equations		Modified ordinates for curve fitting Eq. of Curve $YC \equiv (a/XC) + b$	
	$X_j = z_j/h_o$	$Y_j = H_{1,j}$	$XC_j = -(z_b/h_o - X_j)$	$YC_j = -(H_{1,1} - Y_j)$
1	0.00	0.8939	−0.35	0.0000
2	0.10	0.8890	−0.25	−0.0049
3	0.20	0.8723	−0.15	−0.0216
4	0.30	0.8212	−0.05	−0.0727

The least square approximation criteria yields,
$468.6079\,a - 33.5238\,b - 1.6172 \equiv 0$
$-33.5238\,a - 4.0000\,b + 0.0992 \equiv 0$
The solution of the above equations gives a as 0.0042 and b as 0.0103
The required equation of the curve is, $YC = 0.0042/XC + 0.0103$

and which passes through the co-ordinate $O, H_{NC,1}$ has to be determined. The slope which is thus obtained is to be finally used in the dimensionless form of the density interface relationship to obtain the next approximation of the brine cone elevations. A set of computations for obtaining the equation to the fitted curve and the slope of the tangent line in an iterative manner are illustrated in Tables 1 and 2

49

Table 2 – Sample calculations for determining the slope of the straight line which is tangential to the curve and passes through the ordinate $YRE = H_{NC,1}$

Results Apply for: $(P_r/P_z) (h_o/r_e)^2 \equiv 0.12$; $r_e/r_w \equiv 2,896$; $z_b/h_o \equiv 0.35$; $z_t/h_o \equiv 0.95$
$H_{1,1} \equiv 0.8939$; $YRE \equiv H_{NC,1} \equiv 0.9280$; Tolerance level for convergence, $|YRE\text{-}YRE1| \leqslant 0.0050$
Equation of the curve $YC \equiv 0.0042/XC + 0.0103$
Slope of the tangent line, STL is equal to $-0.0042/(XC)^2$

Trial No.	In-crement of XC	XC	YC	STL	X	Y	$YRE1 = Y\text{-}STL \times X$	$YRE\text{-}YRE1$	$|YRE\text{-}YRE1|$
1		-0.3500	-0.0017	-0.0342	0.0000	0.8923	0.8923	0.0358	0.0358
2	0.1000	-0.2500	-0.0064	-0.0670	0.1000	0.8875	0.8942	0.0338	0.0338
3	0.1000	-0.1500	-0.0176	-0.1862	0.2000	0.8763	0.9135	0.0145	0.0145
4	0.1000	-0.0500	-0.0735	-1.6758	0.3000	0.8204	1.3232	-0.3952	0.3952
5	-0.0500	-0.1000	-0.0316	-0.4190	0.2500	0.8623	0.9671	-0.0391	0.0391
6	-0.0250	-0.1250	-0.0232	-0.2681	0.2250	0.8707	0.9310	-0.0030	0.0030

Required slope STL is equal to -0.2681

respectively. The algorithm for the numerical scheme has been translated into a valid computer programme and integrated in the simulation model.

Numerical Scheme for Truncating the Fresh Water Zone

The brine cone elevations obtained from the numerical scheme of Muskat's graphical procedure and the fresh water heads in the top most row of the grid obtained from the solution of the flow equations are used to modify the hydraulic conductances of the affected branches. In order to retain the same number of rows and columns during all trials of the flow equations, the branches which represent aquifer segments which are removed entirely from the fresh water zone are retained in the grid but deactivated by assigning an extremely low hydraulic conductance value.

The depression in the water table may lead to a reduction in the screen length available for groundwater flow into the well at steady state. This aspect has also been taken care of in the digital simulation model. The flow rates assigned to the nodes representing the well screen are modified in proportion to the reduction in screen length during the beginning of each trial solution of the flow equations. Those nodes which are removed totally from the flow domain are deactivated by assigning a zero discharge value.

The Integrated Simulation Model

The three components described above have been integrated in a single digital

50

simulation model to obtain the steady state stable brine cone position for different aquifer, well and fluid density contrast situations. The brine interface in all cases is initially assumed to be horizontal. The solution of the flow equations and the subsequent application of numerical scheme of Muskat's graphical procedure yield the first approximations of the elevations of the brine cone and elevations of the free surface. After modifying the fresh water zone, the solution of the flow equations and applications of numerical scheme of Muskat's graphical procedure are repeated to obtain the next approximation of the elevations of the brine cone and elevations of the free surface. This iterative procedure is continued till successive solutions of brine cone elevations and free surface elevations are within a pre-scribed tolerance level. A complete listing of the computer program with all user instructions along with sample input and output can be had from the authors on request.

Comparison of Digital Simulation Model Results with Available Solutions

Muskat's Method

The results of brine cone elevations obtained from the digital simulation model after the application of the numerical scheme of Muskat's graphical procedure to the solution of the flow equations at the end of the first trial are identical to the results of brine cone elevations as obtained from Muskat's method. In the digital simulation model, the fresh water zone is successively modified and several trials of solutions of flow equations are made till the brine cone elevations at the beginning and at the end of the trial are within a prescribed tolerance level. Let ZP_i and ZC_i represent the brine cone elevations at the radial distance represented by the ith column during the beginning and at the end of a particular trial solution of the flow equations respectively. The manner in which $\sum_{i=1}^{NC} (ZC_i = ZP_i)$, at the end of each trial decreases with increasing number of trials is an indirect indication of the improvements in estimation of the brine cone elevations from the digital simulation model as compared to Muskat's method. Such results for two simulation runs are presented in Table 3. As a further illustration, the results of non-dimensional elevation of the apex of the brine cone from the digital simulation model for a number of simulation runs at the end of the first trial solution and at the end of the trial solution when convergence is achieved within prescribed tolerance levels are presented in Table 4.

The results indicate that Muskat's method will always result in an under estimation of the brine cone elevations. The results also indicate that the improvements in the estimation of brine cone elevations between successive trial solutions are less pronounced for larger flow net constants and for same flow net constant for conditions of shallower screen bottom. This indicates that the more the anisotropy of the aquifer the lesser will be the error in Muskat's method. On the other hand if the

51

Table 3 – Digital Model Results of Variations of Sums of Differences Between Brine Cone Elevation at the End and Beginning of Each Trial

$$r_e/r_w \equiv 2,896 \; ; \; z_b/h_o = 0.35 \; ; \; z_t/h_o = 0.95$$

	NC $\sum\limits_{i=1} (ZC_i - ZP_i)$ in metres	
Trial No.	$(P_r/P_z)(h_o/r_e)^2 \equiv 0.95$;	$(P_r/P_z)(h_o/r_e)^2 = 3.81$
1	260	170
2	85	40
3	45	15
4	25	5
5	10	0

Note: The elevations of the brine cone ZC_i at the end of the first trial in the digital model are identical to those obtained by Muskat's Method.

Table 4 – Digital model results of apex of brine cone – $r_e/r_w = 2,896$; $z_t/h_o = 1.0$

		Apex of brine cone z_a/h_o		
$(P_r/P_z)(h_o/r_e)^2$	z_b/h_o	At end of first trial	At end of several trials after which freshwater flow zone converges within prescribed tolerance level	Difference between Muskat's Solution of z_a/h_o and Digital Model Solution expressed as a percentage of Muskat's Solution
0.12	0.45	0.325	0.407	25
0.12	0.55	0.390	0.467	20
0.12	0.65	0.451	0.532	18
0.12	0.75	0.505	0.582	15
0.95	0.45	0.290	0.336	16
0.95	0.55	0.343	0.378	10
0.95	0.65	0.390	0.414	6
0.95	0.75	0.428	0.442	3

Note: The elevation of apex of brine cone at the end of the first trial in the digital model are identical to those obtained by Muskat's Method.

anisotropy is less and approaches unity (isotopic conditions), Muskat's method will result in greater errors in estimation of the brine cone elevation. The results from a number of simulation runs also indicated that generally not more than 4 or 5 trial

Table 5 – Comparison of digital and electric analog model results
$(P_r/P_z) (h_o/r_e)^2 \equiv 0.423$; $z_t/h_o \equiv 0.95$; $r_e/r_w \equiv 2,896$

Type of model	z_b/h_o	z_a/h_o	$(\triangle \rho / \rho_f) (h_o/(h_o\text{-}h_w))$	$Q/(h_o P_r(h_o\text{-}h_w))$
Digital	0.35	0.30	0.59	0.53
Analog	0.35	0.30	0.61	0.53
Digital	0.55	0.41	0.22	0.38
Analog	0.55	0.39	0.25	0.37
Digital	0.75	0.51	0.09	0.21
Analog	0.75	0.47	0.09	0.21

runs will be needed in the digital simulation model to obtain the final stable brine cone elevations.

Electric Analog Model

The results obtained from the digital simulation model for a few cases have been compared in Table 5, with the direct electric analog model results of Bennet, Mundorff and Amjad Hussain (1968). It is seen that the results from the two studies compare reasonably well.

Results and Discussion

Model Parameters

The number of columns and rows in the grid were 24 and 11 respectively in all simulation runs. α, r_w, h_o, P_r and z_t were always taken as $\sqrt{2}$, 0.1 m, 100 m, 0.00025 m/sec, and 100 m respectively. In different simulation runs either the anisotropy P_r/P_z of the aquifer or the bottom of well screen z_b were varied. All results apply for $z_t/h_o = 1.0$ and $r_e/r_W = 2,896$. The associated dimensionless parameters, $(P_r/P_z)(h_o/r_e)^2$, $Q/(h_o P_r(h_o\text{-}h_w))$, $(\triangle \rho / \rho_f)(h_o/(h_o\text{-}h_w))$, z_a/h_o and z_b/h_o were computed for each simulation run.

Results from Simulation Runs

The results from the digital simulation model have been consolidated and presented in non-dimensional form in Figs. 3, 4 and 5. They give the variation of non-dimensional apex of the brine cone z_a/h_o, the slope of the non-dimensional form of the density interface relationship $(\triangle \rho / \rho_f) (h_o/(h_o\text{-}h_w))$, and the non-dimensional specific capacity function $Q/(h_o P_r(h_o\text{-}h_w))$, respectively with flow net constant $(P_r/P_z) (h_o/r_e)^2$ for different values of non-dimensional elevation of screen bottom z_b/h_o.
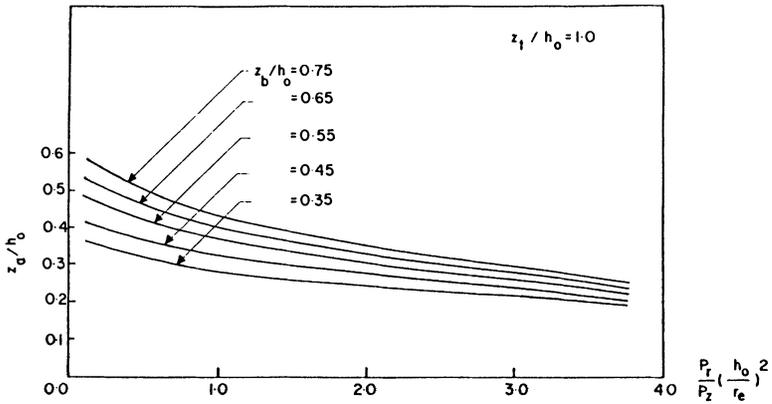
53

Fig. 3. Dimensionless apex of brine cone versus flow net constant for varoius positions of screen bottom.
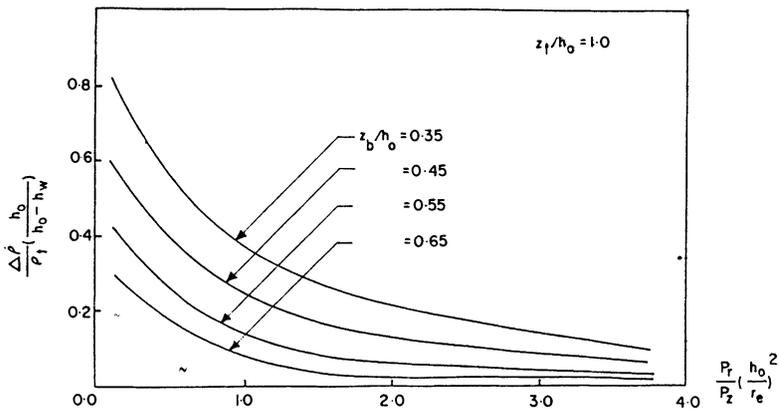

Fig. 4. Slope of non-dimensional form of the equation of density interface relationship versus flow net constant for different positions of screen bottom.

Utility of Results in Non-dimensional Form

The results from a single simulation run since they are presented in a non-dimensional form, can apply equally well for several alternative aquifer well and fluid density contrast situations.

Consider for example the results from the simulation run for which the flownet constant, $(P_r/P_z) (H_o/r_e)^2 = 0.119$ and $z_b/h_o = 0.45$. In this case r_e/r_w is 2,896 and z_t/h_o is 1.0. The results from the simulation run for this case are, $z_a/h_o = 0.41$, $(\Delta \rho/\nu_f) (h_o/(h_o-h_w)) = 0.60$, and $Q/(h_o P_r(h_o-h_w)) = 0.50$. Two alternative situations where the results can apply equally well are presented in Table 6.
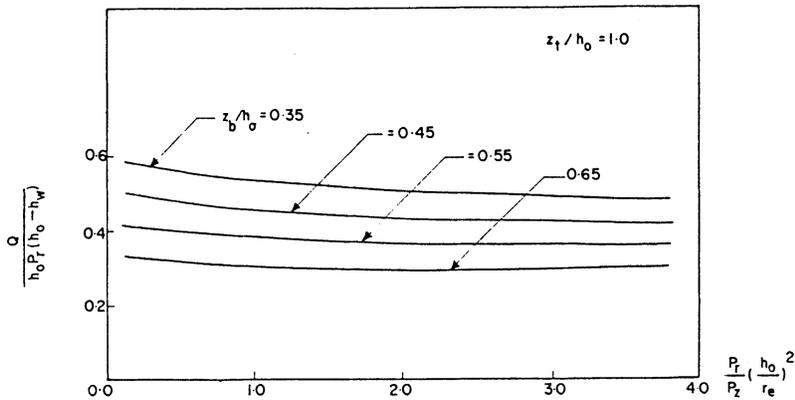
54

Fig. 5. Dimensionless specific capacity function versus flow net constant for various positions of screen bottom.

Table 6 – Alternative situations where the results are equally valid

$(P_r/P_z) (h_o/r_e)^2 \equiv 0.119$; $r_e/r_w \equiv 2.896$

$z_t/h_o = 1.0$; $z_b/h_o \equiv 0.45$

$z_a/h_o = 0.41$; $(\triangle \rho/\rho_f) (h_0/(h_o-h_w)) \equiv 0.60$; $Q/(h_o P_r(h_o-h_w)) \equiv 0.50$

Parameters	Case 1	Case 2
Aquifer		
P_r	0.0025 m/sec.	0.00025 m/sec.
P_r/P_z	1.0	4.0
r_e	289.6 m	289.6 m
h_o	100.0 m	50.0 m
Well		
r_w	0.1 m	0.1 m
z_b	45.0 m	22.5 m
z_t	100.0 m	50.0 m
Fluid Density Contrast		
$\triangle \rho_{\rho_f}$	0.025	0.025
Typical Results		
Maximum permissible discharge, Q	0.025 m^3/sec.	0.013 m^3/sec.
Associated drawdown in well, $h_o - h_w$	4.2 m	2.1 m
Associated apex of brine cone, z_a	*41 m*	*20.5 m*

Field Application of the Model Results

The results obtained from the digital simulation model can find applications in solving field problems related to brine coning beneath partially penetrating wells pumping from the fresh water zone overlying a saline zone. The non-dimensional plots of the results presented in Figs. 3, 4 and 5 form the basis for the applications.

Data Requirement
i) The parameters of the aquifer namely, lateral permeability P_r, and anisotropy P_r/P_z where P_z is vertical permeability.
ii) The geometry of the aquifer in terms of saturated tickness, h_o, and radius of influence r_e.
iii) The geometry of the well in terms of its radius r_w and elevation of the well screen bottom z_b.
iv) The density of the fresh water ρ_f and the density of the underlying saline water, ρ_s. The ratio $\triangle\rho/\rho_f$ is referred to as the density contrast.

The results presented in this paper apply for the situations when the elevation of the top of the well screen is the same as h_o, and the ratio r_e/r_w is 2,896. These will be the commonly encountered conditions in the field. The digital simulation model which has been presented in this paper can be however also utilised to obtain results for alternative elevations of the top of the well screen z_t and r_e/r_w ratios.

Results which can be obtained
i) The maximum permissible discharge Q which can be pumped from the aquifer so that a stable brine cone is established with the apex of the brine cone being below the bottom of the well screen.
ii) The associated elevation of the apex of the stable brine cone z_a.
iii) The associated drawdown in the well, h_o-h_w.

Method of Obtaining the Results
i) The flownet constant, $(P_r/P_z)\ (h_o/r_e)^2$, the non-dimensional elevation of the bottom of the well screen z_b/h_o, and the density contrast $\triangle\rho/\rho_f$ are first computed.
ii) Fig. 3 is used to obtain z_a/h_o for the computed values of $(P_r/P_z)\ (h_o/r_e)^2$ and z_b/h_o. If the plot for the computed value of z_b/h_o is not available in the figure, suitable interpolation may be made. Since the value of h_o and z_a/h_o are known the elevation of the apex of the brine cone z_a can be computed.
iii) Fig. 4 is used to obtain $(\triangle\rho/\rho_f)\ (h_o/(h_o-h_w))$ for the computed values of $(P_r/P_z)\ (h_o/r_e)^2$ and z_b/h_o. Since the values of $\triangle\rho/\rho_f$ and h_o are known, the value of the drawdown within the well $h_o - h_w$ can be calculated.
iv) Fig. 5 is used to obtain the value of $Q/(h_oP_r(h_o-h_w))$ for the computed values of $(P_r/P_z)(h_o/r_e)^2$ and z_b/h_o. Since the values of h_o, P_r and $h_o - h_w$ are known, the value of the maximum permissible discharge Q can be computed.

Conclusions

A digital simulation model has been developed for locating the steady-state brine cone position beneath fresh water wells tapping from the fresh water zone overlying a saline zone in an unconfined anisotropic aquifer. The model facilitates a wide range of aquifer, well and fluid density contrast conditions to be elegantly tackled and is a significant improvement over existing methods of solution to the problem of brine coning. The results from the digital simulation model have been presented in the form of graphs making use of appropriate non-dimensional parameters. A detailed procedure for field applications of the simulation model results has also been discussed. The data requirements for application of the results are the parameters of the aquifer in terms of its lateral permeability and anisotropy, geometry of the aquifer in terms of its saturated thickness and radius of influence, geometry of the well in terms of its radius and elevation of well screen bottom, and parameters of the salt and fresh water in terms of their density contrast. The results that can be obtained are the maximum permissible discharge which can be pumped from the aquifer so that a stable brine cone is established with the apex of the brine cone being below the bottom of the well screen, the elevation of the stable brine cone, and the associated steady state drawdown in the well.

References

Bear and Dagan (1968) Solving the problem of local interface upcoming in a coastal aquifer by the method of small perturbations, *Journal of Hydraulic Research, Vol. 1*.

Bennet, G. D., Mundroff, M. J., and Hussain, S. Amjad (1968) Electric analog studies of brine coning beneath fresh water wells in the Punjab region, West Pakistan, U.S. Geological Survey Water-Supply Paper, 1608-09.

Hubbert, M. K. (1940) The theory of ground water motion, *Journal of Geology, Vol. 48*, No. 8 part 1.

Kemblowski (1985) Saltwater-freshwater transient upcoming – an implicit boundary element solution, *Journal of Hydrology, Vol. 78*.

Lakshminarayana, V., and Rajagopalan, S. P. (1977) Digital model studies of steady-state radial flow to partially penetrating wells in alluvial plains, *Groundwater, Vol. 15*, No. 3, pp 223-230.

Muskat, Morris (1937) The flow of homogeneous fluids through porous media, Repr. 1964, Anna Arbor, J. W. Edwards, Inc., pp. 487-490.

Muskat, Morris (1949) *Physical principles of oil production*, New York, McGraw Hill Co. pp 226-236.

Neuman, S. P. (1974) Effect of partial penetration of flow in unconfined aquifers considering delayed gravity response, *Water Resources Research, Vol. 10*, No. 3, pp 303-312.

Prickett, T. A., and Lonnquist, C. G. (1971) Selected digital computer techniques for groundwater resources evaluation, Illinois State Water Survey Bulletin, p 62.

Acknowledgements

Address:
Groundwater Division,
CWRDM,
Calicut 673 571,
Kerala,
India.

58